### Title

Input-specific control of reward and aversion in the ventral tegmental area.




### Journal

Nature, 491(7423)

### ISSN

0028-0836



### Authors

Lammel, Stephan
Lim, Byung Kook
Ran, Chen
et al.



### Publication Date

2012-11-01

### DOI

10.1038/nature11527

Peer reviewed

HHS Public Access

Author manuscript

*Nature*. Author manuscript; available in PMC 2013 May 08.

Published in final edited form as:

*Nature*. 2012 November 8; 491(7423): 212–217. doi:10.1038/nature11527.

# Input-specific control of reward and aversion in the ventral tegmental area

**Stephan Lammel**[1,*], **Byung Kook Lim**[1,*], **Chen Ran**[1], **Kee Wui Huang**[1], **Michael J. Betley**[1], **Kay Tye**[3], **Karl Deisseroth**[2], and **Robert C. Malenka**[1]

[1]Nancy Pritzker Laboratory, Department of Psychiatry and Behavioral Sciences, Stanford University School of Medicine, 265 Campus Drive, Stanford CA 94305, USA

[2]Departments of Bioengineering and Psychiatry, Stanford University, Stanford CA 94305, USA

[3]Picower Institute for Learning and Memory, Department of Brain and Cognitive Sciences, Massachusetts Institute of Technology, Cambridge, MA 02139, USA

## Abstract

Ventral tegmental area (VTA) dopamine neurons play important roles in adaptive and pathological brain functions related to reward and motivation. It is unknown, however, if subpopulations of VTA dopamine neurons participate in distinct circuits that encode different motivational signatures and whether inputs to the VTA differentially modulate such circuits. Here we show that because of differences in synaptic connectivity activation of inputs to the VTA from the laterodorsal tegmentum and the lateral habenula elicit reward and aversion in mice, respectively. Laterodorsal tegmentum neurons preferentially synapse on dopamine neurons projecting to nucleus accumbens lateral shell while lateral habenula neurons synapse primarily on dopamine neurons projecting to medial prefrontal cortex as well as on GABAergic neurons in the VTA tail. These results establish that distinct VTA circuits generate reward and aversion and thereby provide a novel framework for understanding the circuit basis of adaptive and pathological motivated behaviors.

---

The functional roles of VTA dopamine (DA) neurons have received great attention because they are the primary source of DA in target structures such as the medial prefrontal cortex (mPFC) and nucleus accumbens (NAc), which play important roles in a broad range of motivated behaviors and neuropsychiatric disorders[1-3]. Although DA neuron activity often correlates with a reward prediction error (i.e. the difference between expected and actual rewards) these cells also can signal aversion, saliency, uncertainty and novelty[2, 3]. They are

---



Correspondence to: R. Malenka Department of Psychiatry and Behavioral Sciences, 265 Campus Drive, Room G1021 Stanford University School of Medicine Stanford, CA 94305 Tel. 650-724-2730 Fax. 650-724-2753 malenka@stanford.edu.

*These authors contributed equally

**Author Contributions** S.L., B.K.L. and R.C.M. designed the study, interpreted results and wrote the paper. S.L. and B.K.L. performed stereotactic injections, optogenetic experiments and electrophysiology. S.L., C.R., M.J.B. and K.W.H. performed immunohistochemistry. B.K.L. and K.W.H. generated viruses. K.T. and K.D. provided optogenetics training and resources. All authors edited the paper.

**Full Methods** and any associated references are available in the on-line version of the paper.

heterogeneous in their anatomical location, targets to which they project, electrophysiological properties and several molecular features[2, 4-6]. In addition, the VTA receives both excitatory and inhibitory input from distributed brain areas[2, 7, 8]. Thus different subpopulations of VTA DA and GABAergic neurons may subserve different functions[1, 2, 4-7, 9-15] but little is known about the afferent control of their activity and the circuits in which they are embedded.

Here we study the function and synaptic connectivity of two major inputs to the VTA from the laterodorsal tegmentum (LDT) and the lateral habenula (LHb). By achieving optogenetic control of LDT and LHb neurons/axons that project directly to VTA and combining *in vivo* viral-mediated and anatomical tracing methods with *ex vivo* electrophysiology during stimulation of specific VTA inputs, we define critical differences in the neural circuits responsible for this optogenetic control of reward and aversion.

## Inputs to the VTA from LDT and LHb

To identify unambiguously the afferent inputs to the VTA, we used a rabies virus in which the glycoprotein is replaced by EGFP (RV-EGFP)[16]. Consistent with recent results[17], injection of RV-EGFP into the VTA resulted in expression of EGFP in diverse brain areas with large clusters of EGFP-expressing cells in the PFC, NAc, lateral hypothalamus, LHb and LDT (Supplementary Fig. 1). We focused on inputs to the VTA from the LDT and LHb because both play roles in motivated behaviors by influencing VTA neuronal activity and the consequent release of DA in target structures[2, 7, 18]. EGFP-positive LDT neurons expressed markers for both glutamatergic neurons (the glutamate transporter EAAC1) and cholinergic neurons (choline acetyltransferase; ChAT) (Supplementary Fig. 2)[19,20]. However, while 95% of LDT neurons projecting to VTA expressed EAAC1, only ~7% expressed ChAT. LHb neurons are excited by the absence of an expected reward[18] and likely send direct inputs to GABAergic cells in the tail of the VTA, the rostromedial tegmental nucleus (RMTg)[21, 22], that inhibit VTA DA neurons[23-26]. EGFP-positive LHb neurons were immunopositive for EAAC1 but not for ChAT (Supplementary Fig. 2) indicating that LHb neurons projecting to VTA are glutamatergic[8].

To visualize fibers within the VTA from LDT and LHb we injected the anterograde tracer *Phaseolus vulgaris leucoagglutinin* (PHA-L). It was apparent that the density of LDT and LHb inputs differed between VTA subregions in which different subpopulations of DA neurons reside[4, 5]. To test this conclusion, we simultaneously retrogradely labeled DA projection neurons and anterogradely labeled LDT or LHb fibers (Fig. 1a, h). Injection of PHA-L into LDT and RV expressing tdTomato (RV-tdTomato) into NAc lateral shell (Fig. 1a, b) revealed that RV-tdTomato cells were predominantly located in lateral VTA (Fig. 1c) that in close proximity contained LDT terminals as well as TH-immunopositive processes (Fig.1d, e). More modest PHA-L labeling was observed in medial VTA (Fig. 1f) and substantia nigra (SN; Fig. 1g). In contrast, injection of PHA-L into LHb and RV-tdTomato into mPFC (Fig. 1h, i) revealed RV-tdTomato cells mainly in medial VTA (Fig. 1j) in close proximity to LHb terminals and TH-immunopositive processes (Fig. 1k, l). There was minimal PHA-L labeling of LHb inputs in the lateral VTA (Fig. 1m) or SN (Fig. 1n) but as expected[21, 22] PHA-L terminals were present in RMTg adjacent to GABAergic neurons

(Supplementary Fig. 3). In additional experiments, we injected fluorescent retrobeads into NAc lateral shell or mPFC and labeled LDT or LHb inputs with PHA-L, respectively. A similar anatomical distribution of pre- and postsynaptic elements was observed (Supplementary Fig. 3).

## Input specific control of reward and aversion

These anatomical results suggest that LDT and LHb inputs preferentially terminate in different VTA subregions adjacent to DA neuron subpopulations that project to different target structures (NAc lateral shell versus mPFC) and may subserve different behavioral functions[5, 6]. To address functional differences in these inputs, we generated a RV expressing the light-activated ion channel ChR2 fused to enhanced yellow fluorescent protein (EYFP, RV-ChR2) (Supplementary Fig. 4) and tested the consequences of activation of LDT-VTA and LHb-VTA pathways in a conditioned place preference (CPP) assay by injecting RV-ChR2 or RV-EGFP into VTA and implanting an optical fiber over LDT or LHb (Fig. 2a, b). Using a three day protocol (Fig. 2c), phasic stimulation of LDT neurons projecting to VTA on day 2 caused a strong CPP on day 3 (Fig. 2d, f, g), while phasic stimulation of LHb neurons projecting to VTA caused a strong conditioned place aversion (CPA) (Fig. 2e-g). Moreover, after the day 3 testing procedure (Post-Test 1), stimulating LDT neurons whenever animals were in the chamber in which they were conditioned on day 2 (Day 3, Post-Test 2) caused a further increase in CPP (Fig. 2h) whereas stimulating LHb neurons did not further enhance CPA (Fig. 2h). (See Supplementary Fig. 5 for, non-normalized behavioral results.)

Additional results indicate that the effects of stimulating LDT and LHb neurons projecting to VTA were specific and due to driving activity in distinct populations of VTA neurons. First, animals that received intra-VTA injections of RV-EGFP exhibited no behavioral effects of phasic optical stimulation in LDT and LHb (Fig. 2f-h; Supplementary Fig. 5). Furthermore, low frequency stimulation of ChR2 in LDT and LHb had no effects in CPP/CPA assays (Fig. 2i; Supplementary Fig. 5). Second, non-stimulated animals showed no preference for either chamber (Supplementary Fig. 4) and there was no effect of the optogenetic manipulations on time spent in the central chamber (Supplementary Fig. 6). Third, stimulation of LDT and LHb neurons projecting to VTA had no effects on open field assays of anxiety or locomotor activity (Supplementary Fig. 6, 7). Fourth, the placement of optical fiber in LDT and LHb was confirmed in all animals (Supplementary Fig. 7). Fifth, VTA DA neuron activation following LDT and LHb stimulation was quantified by assaying the proportion of TH-immunopositive and TH-immunonegative neurons that expressed the activity-dependent immediate early gene c-fos (Supplementary Fig. 8). Following LDT stimulation, ~40% of DA neurons in lateral VTA expressed c-fos whereas in medial VTA three-fold less DA neurons expressed c-fos. Activation of LHb inputs to the VTA caused an opposite pattern of c-fos expression: ~12% of DA neurons in medial VTA were c-fos-positive whereas <2% of DA neurons in lateral VTA expressed c-fos. Importantly, ~80% of non-DA neurons in the RMTg were c-fos-positive following LHb stimulation (Supplementary Fig. 8).

Based on these results we hypothesized that LHb inputs drive DA neurons in the medial posterior VTA that project to mPFC[4-6]. To test this prediction, we activated LHb inputs to VTA in animals in which medial VTA neuron subpopulations that project to different targets were identified by the presence of fluorescent retrobeads (Supplementary Fig. 8). In medial VTA, ~80% of neurons projecting to mPFC were c-fos-positive following LHb stimulation. In contrast, <10% of neurons projecting to NAc medial shell that are located in medial VTA[4-6] expressed c-fos following LHb stimulation.

Although the c-fos results confirm that stimulation of LDT and LHb neurons activated neurons in the VTA, axon collaterals of LDT and LHb neurons may project to other brain regions, activation of which mediated the observed CPP and CPA. To address this possibility, we injected adeno-associated viruses expressing ChR2-EYFP (AAV-ChR2) into LDT or LHb and stimulated axons of infected neurons using light application directly in the caudal VTA and RMTg (Supplementary Fig. 9). This produced robust CPP following intra-VTA LDT axonal stimulation and robust CPA following intra-VTA LHb axonal stimulation (Supplementary Fig. 9, 10). A limitation of these experiments is that intra-VTA activation of LDT and LHb axons may cause antidromic activation of axon collaterals projecting to other brain regions. To address this possibility, we injected RV-EGFP or RV-tdTomato into VTA and the other virus into brain regions that receive inputs from LDT or LHb[27, 28]. If single LDT or LHb neurons projecting to VTA send collaterals to these other brain regions, the neurons will express both fluorophores. An extremely small number of LDT and LHb neurons projecting to other structures (i.e. ventral pallidum, lateral septum, lateral hypothalamus, mPFC, mediodorsal thalamic nucleus, and supraoculomotor central grey) expressed both fluorophores (Supplementary Fig. 11), suggesting that almost all of these neurons project solely to VTA/RMTg. As a positive control we injected one RV into VTA and the other into ventral pallidum and found dorsal raphe neurons (~20%), which are known to project to these two structures[29], expressed both EGFP and tdTomato (Supplementary Fig. 11). We also injected RVs into VTA and either LDT or LHb and examined labeling of cells in the other structure. Our results confirm that LDT and LHb have reciprocal anatomical connections[28] but the cells providing these projections do not project to VTA (Supplementary Fig. 11).

## Synaptic connectivity of LDT and LHb inputs

The results thus far suggest that LDT and LHb inputs activate distinct populations of VTA and RMTg neurons and that this leads to reward and aversion, respectively. To address the specific synaptic connectivity of these inputs, we injected AAV-ChR2 into LDT and fluorescent retrobeads into target structures of VTA DA neurons (Fig. 3a; Supplementary Fig. 12). 8-12 weeks following these injections, ChR2–EYFP was expressed adjacent to VTA DA neurons projecting to NAc lateral shell (Fig. 3b) and its levels were significantly higher in the lateral VTA (Supplementary Fig. 13). To determine the DA neuron populations upon which LDT inputs directly synapse, we made whole-cell recordings from retrogradely labeled DA neurons projecting to the NAc lateral and NAc medial shell as well as non-labeled DA SN neurons (Fig. 3c, d, f). On average, optical stimulation of LDT fibers generated larger excitatory postsynaptic currents (EPSCs) in DA neurons projecting to NAc lateral shell than in DA neurons projecting to medial shell or DA neurons in SN (Fig. 3g), all

recorded in the same sets of slices. The EPSCs in DA neurons projecting to NAc lateral shell were blocked by an AMPA receptor antagonist (CNQX, 10 μM; Fig. 3c) indicating that LDT fibers released glutamate. Importantly, stimulation of LDT inputs generated EPSCs (> 10 pA) in 100% of DA neurons projecting to NAc lateral shell but only in ~30-40% of DA neurons projecting to NAc medial shell or in SN (Fig. 3h). Furthermore, only ~10% of DA neurons projecting to mPFC yielded EPSCs (Fig. 3e, g, h).

The same methodology (Fig. 4a; Supplementary Fig. 12) revealed that LHb inputs synapse on a different subpopulation of VTA DA neurons as well as on GABAergic cells in the RMTg. ChR2-EYFP expressing fibers from the LHb were found in medial posterior VTA in close proximity to DA neurons projecting to mPFC as well as in the RMTg (Supplementary Fig. 12, 13). Importantly, light-evoked EPSCs were generated in 100% of DA neurons projecting to mPFC as well as GABAergic RMTg neurons whereas detectable EPSCs were not generated in DA neurons projecting to NAc medial shell or NAc lateral shell nor in SN neurons (Fig. 4b-g). Since LHb inputs preferentially synapse on NAc DA neurons projecting to mPFC and RMTg GABAergic cells, we predicted that LHb inputs may inhibit DA neurons projecting to NAc lateral shell via feed-forward inhibition. Indeed, in ~60% of DA neurons projecting to NAc lateral shell stimulation of LHb inputs evoked IPSCs (Fig. 4h, i). In contrast, stimulation of LHb axons did not generate detectable IPSCs in DA neurons projecting to NAc medial shell (Fig. 4h).

These results suggest that LDT and LHb inputs to VTA preferentially activate distinct populations of DA neurons that project to different target structures and that in addition, LHb inputs activate GABAergic cells in RMTg and perhaps within the VTA itself. Such differences in connectivity can explain the different behavioral consequences of LDT and LHb stimulation (Fig. 2). To further test these conclusions, we generated AAVs expressing a double floxed RV glycoprotein (AAV-DIO-RVG) and infected the VTA in TH-Cre mice so that glycoprotein was only expressed in DA neurons (Fig. 5a). Two weeks later, RV-EGFP and RV-tdTomato were injected into mPFC and NAc lateral shell, respectively (Fig. 5a, b). Because RV-EGFP and RV-tdTomato lack RV glycoprotein, expression of EGFP and tdTomato is restricted to initially infected cells[16]. However, in VTA DA neurons projecting to these targets (Fig. 5c), transcomplementation with RV glycoproteins occurs and allows RV-EGFP and RV-tdTomato to spread retrogradely, thus labeling cells that synaptically contact the DA neurons. After RV injections, cells in LDT were clearly labeled with tdTomato with almost no cells expressing EGFP (tdTomato, n=18.75 ± 7.12 cells per animal, EGFP, n=1.25 ± 0.75, n=4 mice; Fig. 5d) while LHb cells were clearly labeled with EGFP with almost no cells expressing tdTomato (EGFP, 8.25 ± 3.44 cells; tdTomato, 0.5 ± 0.22, n=4 mice; Fig. 5e). When AAV-DIO-RVG was not injected into VTA prior to RV injections, no tdTomato-positive or EGFP-positive cells in LDT or LHb, respectively, were observed (n=3 mice) (Fig. 5f, g). These results confirm that LDT neurons preferentially synapse on VTA DA neurons projecting to NAc lateral shell and LHb neurons preferentially synapse on VTA DA cells projecting to mPFC.

## Effects of DA receptor antagonists in mPFC and NAc lateral shell

Activation of VTA GABAergic cells alone can elicit CPA[13] and disrupt reward consummatory behavior[15]. These results raise the question of whether activation of DA neurons projecting to mPFC is necessary for the CPA elicited by activation of LHb inputs to VTA and RMTg. To address this question, we infused the D1 dopamine receptor antagonist SCH23390 into mPFC immediately prior to stimulating LHb neurons projecting to VTA and RMTg (Fig. 5h). This manipulation, which does not impair cocaine CPP[30], prevented the occurrence of CPA, which was elicited in control animals that received vehicle injections into mPFC (Fig. 5i, j; Supplementary Fig. 14). Similarly, infusion of D1 and D2 receptor antagonists into NAc lateral shell, but not infusion of vehicle, prevented the CPP elicited by activation of LDT neurons projecting to VTA (Fig. 5k-m, Supplementary Fig. 14). Control experiments revealed that infusion of DA receptor antagonists alone into either the mPFC or NAc lateral shell did not elicit CPP or CPA compared to animals that received vehicle infusions ($n = 4$ mice in each group; $p > 0.05$ Mann-Whitney U-tests). These results provide further evidence that activation of different subpopulations of VTA DA neurons and the consequent release of DA in different target structures are necessary for mediating the reward and aversion generated by activation of LDT and LHb inputs, respectively.

## Concluding remarks

A fundamental task of the mammalian brain is to assign emotional/motivational valence to environmental stimuli by determining whether they are rewarding and should be approached or are aversive and should be avoided. Internal stimuli also are assigned emotional/motivational valence and prevalent brain disorders, such as addiction and depression, involve pathological dysfunction in the performance of these tasks. Although VTA DA neurons play a role in reward-dependent behaviors[1-3, 7, 10, 12, 14, 31, 32] and inhibition of VTA DA neurons by GABAergic neurons contributes to reward prediction error calculations and promotes behaviors associated with aversion[10, 12, 13, 15], the detailed circuits within the VTA that mediate reward and aversion and their control by upstream brain areas have not been defined. By combining virus-mediated tracing, synaptic electrophysiology and *in vitro* and *in vivo* optogenetic manipulations, we have presented evidence that two major inputs to the VTA from the LDT and LHb trigger reward- and aversion-associated behaviors, respectively, via activation and perhaps disynaptic inhibition of distinct subpopulations of VTA DA neurons that project to different target structures. These findings suggest that there are several subpopulations of VTA DA neurons embedded in distinct circuits that contribute to different behavioral functions (Fig. 5n). DA neurons projecting to mPFC may be the primary subpopulation of DA neurons that are preferentially activated by aversive stimuli although these neurons likely subserve other important functions[33]. On the other hand, DA neurons projecting to NAc lateral shell may primarily signal reward and perhaps salience[2, 5]. This hypothesis is consistent with studies measuring the release of DA in target structures following stimulation of LDT and LHb as well as recent optogenetic manipulations of VTA DA neuron activity[10, 19, 31, 32, 34].

Although LDT and LHb inputs activate different cell populations in VTA and RMTg, it is likely that these distinct “circuits” do not routinely function in isolation. They interact with

one another anatomically[28] (Supplementary Fig. 11) and functionally (Figure 4). Indeed, stimuli can have both rewarding and aversive qualities simultaneously and these qualities can change depending on the context. Thus, LDT and LHb inputs to VTA and RMTg can be conceptualized as belonging to a more complex global brain system that assigns motivational valence or value to external and internal stimuli. Further elucidation of the detailed synaptic connectivity of LHb inputs to VTA may be particularly interesting in the context of the potential role of LHb in psychiatric disorders such as depression and schizophrenia[18, 35-37]. Overactivity of LHb neurons would be expected to drive depressive symptoms such as anhedonia while LHb pathology in schizophrenia may contribute to the cognitive symptoms that are associated with PFC dysfunction[37].

## METHODS (for online version of paper)

### Animals

Male adult (10-12 weeks of age) C57Bl6 (Charles River) or TH-Cre [B6.Cg-Tg(Th-cre)1Tmd/J; Jackson Laboratory] mice were used for all experiments. All procedures complied with the animal care standards set forth by the National Institutes of Health and were approved by Stanford University's Administrative Panel on Laboratory Animal Care.

### Virus Generation

The adeno-associated viruses (AAVs) used in this study were generated as previously described[38] either by the Deisseroth lab (AAV-ChR2) or the Stanford Neuroscience Gene Vector and Virus Core (AAV-DIO-RVG). Rabies virus (RV) was generated from a full length cDNA plasmid containing all components of RV (SAD L16; gift from Dr. Karl-Klaus Conzelmann, University of Munich, Germany)[39]. We replaced the rabies virus glycoprotein with EGFP, tdTomato or ChR2-H134R fused to EYFP to generate RV expressing EGFP (RV-EGFP), tdTomato (RV-tdTomato), or ChR2-H134R (RV-ChR2). To harvest RV from this cDNA we used a modified version of published protocols[39, 40]. Briefly, HEK293T cells were transfected with a total of 6 plasmids; 4 plasmids expressing the RV components pTIT-N, pTIT-P, pTIT-G, and pTIT-L; one plasmid expressing T7 RNA polymerase (pCAGGS-T7), and the aforementioned glycoprotein-deleted RV cDNA plasmid expressing EGFP, tdTomato, or ChR2. For the amplification of RV, the media bathing these HEK293T cells was collected 3-4 days posttransfection and moved to baby hamster kidney (BHK) cells stably expressing RV glycoprotein (BHK-B19G)[40]. After three days, the media from BHK-B19G cells was collected, centrifuged for 5 min at 3,000 × g to remove cell debris, and concentrated by ultracentrifugation (55,000 × g for 2 hr). Pellets were suspended in DPBS, aliquoted and stored at -80°C. The titer of concentrated RV was measured by infecting HEK293 cells and monitoring fluorescence. Plasmids expressing the RV components were gifts from Dr. Karl-Klaus Conzelmann and Dr. Ian Wickersham (Massachusetts Institute of Technology, MA). BHK cells stably expressing B19G were a gift from Dr. Edward Callaway (Salk Institute, La Jolla, CA).

### Stereotaxic injections and optic fiber/cannula implantations

As previously described[4, 5], all stereotaxic injections were performed under general ketamine-medetomidine anesthesia and using a stereotaxic instrument (Kopf Instruments).

Adult (10-12 weeks; 25-30g) male C57BL/6 and TH-Cre mice were group-housed until surgery. Mice were maintained on a 12:12 light cycle (lights on at 07:00). For retrobead labeling (100 nl; LumaFluor Inc., Naples, FL) mice were injected unilaterally with fluorescent retrobeads in the nucleus accumbens (NAc) lateral shell (bregma 1.45 mm; lateral 1.75 mm; ventral 4.0 mm), NAc medial shell (bregma 1.78 mm; lateral 0.5 mm; ventral 4.1 mm), or medial prefrontal cortex (mPFC) (two injections at four different sites: bregma 1.95 mm, 2.05 mm, 2.15 mm, and 2.25 mm; lateral 0.27 mm; ventral 2.1 mm and 1.6 mm; injected total volume in mPFC: 400 nl; the target area was the prelimbic and infralimbic cortex) using a 1 µl Hamilton syringe (Hamilton, Reno, NV). Note that these empirically derived stereotaxic coordinates do not precisely match those given in the mouse brain atlas (Franklin and Paxinos, 2001), which we used as references for the injection-site images. On average, the caudo-rostral axis appeared to be approximately shifted caudally by 400 µm. Little labeling was observed in the pipette tract (i.e. cingulate and motor cortices for mPFC injections or in the dorsal striatum for NAc lateral shell injections). To allow adequate time for retrograde transport of the Retrobeads into the somas of midbrain DA neurons, minimal survival periods prior to sacrifice depended on the respective injection areas: NAc lateral shell, 3 days; NAc medial shell, 14 days; and mPFC, 21 days. For viral infections a small amount of concentrated rabies virus (RV) solution (0.5-1 µl of RV-EGFP, RV-tdTomato or RV-ChR2) or AAV-DIO-RVG or AAV-ChR2-EYFP was injected unilaterally in the LDT (bregma -5.0 mm; lateral 0.5 mm; ventral 3.0 mm) or LHb (bregma -1.58 mm; lateral 0.4 mm; ventral 2.65 mm) or into the VTA (bregma -3.4 mm; lateral 0.35 mm; ventral 4.0 mm) or mPFC or NAc lateral shell (same coordinates as for retrobead injections) using a syringe pump (Harvard Apparatus, MA) at a slow rate (100-150 nl/min). The injection needle was withdrawn 5 min after the end of the infusion.

For the dual RV injections (Supplementary Fig. 11), one virus (RV-EGFP or RV-tdTomato) was injected into the VTA and the other was injected into either the ventral pallidum (bregma 0.62 mm; lateral 1.10 mm; ventral 4.75 mm), lateral septum (bregma 0.62 mm; lateral 0.35 mm; ventral 3.0 mm), lateral hypothalamus (bregma -0.94 mm; lateral 1.00 mm; ventral 4.75 mm), mPFC (two injections at four different sites: bregma 1.95 mm, 2.05 mm, 2.15 mm, and 2.25 mm; lateral 0.27 mm; ventral 2.1 mm and 1.6 mm), mediodorsal thalamic nucleus (bregma -1.22 mm; lateral 0.25 mm; ventral 3.25 mm) or supraoculomotor central grey (bregma -4.04 mm; lateral 0.3 mm; ventral 2.7 mm). For anterograde labeling of LDT and LHb terminals in the VTA the anterograde tracer *Phaseolus vulgaris leucoagglutinin* (PHA-L; 50 nl; 2.5% in 0.01 M phosphate buffer; Vector, Burlingame, CA) was injected into the LDT or LHb (same coordinates as for virus injections). The survival period for the PHA-L injected animals was 3 weeks and for the AAV-ChR2 injected animals 8-12 weeks.

For behavioral experiments mice that were injected with RV-EGFP or RV-ChR2 in the VTA received unilateral implantation of a doric patch-cord chronically implantable fiber (NA=0.22; Doric lenses, Quebec, Canada) over the LDT (bregma -5.0 mm, lateral 0.5 mm, ventral 2.0 mm) or LHb (bregma -1.58 mm, lateral 0.4 mm, ventral 2.0 mm). One layer of adhesive cement (C&B metabond; Parkell, Edgewood, NY) followed by cranioplastic cement (Dental cement; Stoelting, Wood Dale, IL) was used to secure the fiber guide system

to the skull. After 20 min, the incision was closed with a suture and tissue adhesive (Vetbond; Fisher, Pittsburgh, PA). The animal was kept on a heating pad until it recovered from anesthesia. For intra-VTA stimulation of LHb or LDT axon terminals, AAV-ChR2 was injected into LHb or LDT, respectively. 10 weeks following the virus injection a doric optic fiber was implanted unilaterally over the caudal medial VTA for stimulation of LHb axon terminals (bregma -3.4 mm; lateral 0.35 mm; ventral 3.6 mm) and over the lateral VTA for stimulation of LDT axon terminals (bregma -3.4 mm; lateral 0.5 mm; ventral 3.6 mm). Behavioral experiments were performed 2 weeks after the implantation. For microinjection of DA receptor antagonists into the mPFC or NAc lateral shell a guide cannula (PlasticOne, Roanoke, VA) was implanted directly over the ipsilateral mPFC (bregma: 2.2 mm; lateral 0.3 mm; ventral -2.0 mm) or NAc lateral shell (bregma: 1.45 mm; lateral 1.75 mm; ventral 4.0 mm) of the mice in which RV-ChR2 injection into the VTA and the implantation of doric optic fibers were made. Optical fiber and cannula placements were confirmed in all animals. Although placements varied slightly from mouse to mouse, behavioral data from all mice were included in the study.

## Electrophysiology

Mice were deeply anaesthetized with pentobarbital (200 mg/kg ip; Ovation Pharmaceuticals, Deerfield, IL). Coronal midbrain slices (250 μm) were prepared after intracardial perfusion with ice-cold artificial cerebrospinal fluid (ACSF) containing elevated sucrose (in mM): 50 sucrose, 125 NaCl, 25 $NaHCO_3$, 2.5 KCl, 1.25 $NaH_2PO_4$, 0.1 $CaCl_2$, 4.9 $MgCl_2$, and 2.5 glucose (oxygenated with 95% $O_2$/5% $CO_2$). After 90 min of recovery, slices were transferred to a recording chamber and perfused continuously at 2-4 ml/min with oxygenated ACSF (125 NaCl, 25 $NaHCO_3$, 2.5 KCl, 1.25 $NaH_2PO_4$, 11 glucose, 1.3 $MgCl_2$, and 2.5 $CaCl_2$) at ~30 °C. For recording of excitatory postsynaptic currents (EPSCs) picrotoxin (50 μM, Sigma) was added to block inhibitory currents mediated by $GABA_A$ receptors. The internal solution contained (in mM): 117 $CsCH_3SO_3$, 20 HEPES, 0.4 EGTA, 2.8 NaCl, 5 TEA, 4 MgATP, 0.3 NaGTP, 5 QX314, 0.1 Spermine, and 0.1% neurobiotin. For recording of inhibitory postsynaptic currents (IPSCs) the internal solution contained (in mM): 130 CsCl, 1 EGTA, 10 HEPES, 2 MgATP, 0.2 NaGTP, and 0.1% neurobiotin (for both internal solutions pH 7.35, 270–285 mOsm). Patch pipettes (3.8-4.4 MΩ) were pulled from borosilicate glass (G150TF-4; Warner Instruments).

Labeled DA neurons were visualized with a 40x water-immersion objective on an upright fluorescent microscope (BX51WI, Olympus USA) equipped with infrared-differential interference contrast (IR-DIC) video microscopy and epifluorescence (Olympus USA) for detection of retrobeads. ChR2 was stimulated by flashing 473 nm light (5 ms pulses; 0.1Hz; 1-2 mW) through the light path of the microscope using a ultrahigh-powered LED powered by an LED driver (Prizmatix, Modiin Ilite, Israel) under computer control. The light intensity of the LED was not changed during the experiments and the whole slice was illuminated. A dual lamp house adapter (Olympus USA) was used to switch between fluorescence lamp and LED light source. Excitatory postsynaptic currents (EPSCs) were recorded in whole-cell voltage clamp (Multiclamp 700B, Molecular Devices, CA, USA), filtered at 2 KHz, digitized at 10 KHz (ITC-18 interface, HEKA) and collected on-line using custom IgorPro software (Wavemetrics, Lake Oswego, OR, USA). Series resistance (15-25

MΩ) and input resistance were monitored on-line with a 4 mV hyperpolarizing step (50 ms) given with each afferent stimulus. VTA/SN and RMTg neurons were voltage-clamped at -70 mV and EPSC or IPSC amplitudes were calculated by measuring the peak current from the average EPSC or IPSC response from 10-15 consecutive sweeps.

For pharmacological characterization light-evoked EPSCs or IPSCs were recorded for 5 min followed by bath perfusion of 10 μM CNQX (Tocris Bioscience, Ellisville, MI, USA) or 50 μM picrotoxin (Sigma) for an additional 10 min, respectively. 10-15 consecutive sweeps pre- and post-drug were averaged and peak EPSCs or IPSCs amplitudes were then measured. For detection of IPSCs, DA cells were recorded from the caudal VTA in slices that contained the RMTg. For determination of DA or GABAergic phenotype, neurons were filled with neurobiotin (Vector, Burlingame, CA, USA) during the patch clamp experiment, then fixed in 4% PFA and 24h later immunostained for TH or GAD67. Approximately 80% of all whole-cell patch clamped neurons could be successfully recovered. The DA phenotype or GABAergic phenotype (in the RMTg) was confirmed in all of these neurons.

## Immunohistochemistry

Immunohistochemistry and confocal microscopy were performed as described previously[4, 5]. Briefly, after intracardial perfusion with 4% paraformaldehyde in PBS, pH 7.4, the brains were post-fixed overnight and coronal midbrain slices (50 or 100 μm) were prepared. The primary antibody used were mouse anti-tyrosine hydroxylase (TH) (1:1000; Millipore, Temecula, CA, USA), rabbit anti-tyrosine hydroxylase (TH) (1:1000; Calbiochem, San Diego, CA, USA), rabbit anti-PHA-L (1:1000; Vector, Burlingame, CA, USA), goat anti-glutamate transporter (EAAC1; 1:1000; Millipore), rabbit anti-ChAT (1:200; Millipore), mouse anti-GAD67 (clone 1G10.2; 1:500; Millipore), rabbit anti-c-fos (1:500, Calbiochem) and rabbit anti-NeuN (1:1000; Millipore). The secondary antibodies used were Alexa Fluor488 anti-rabbit, AlexaFluor546 anti-goat, AlexaFluor546 anti-rabbit, AlexaFluor546 anti-mouse, Alexa Fluor647 anti-rabbit, Alexa Fluor647 anti-mouse (all 1:750), AlexaFluor488 streptavidin (1:1000) (all Molecular Probes, Eugene, OR). Image acquisition was performed with a confocal system (Zeiss LSM510) using 10x, 40x or 63x objectives and on a Zeiss AxioImager M1 upright widefield fluorescence/DIC microscope with CCD camera using 2.5x and 10x objectives. Images were analyzed using the Zeiss LSM Image Browser software and ImageJ software.

For quantification of ChR2-EYFP fluorescence intensity and quantification of c-fos-positive cells, confocal images were acquired using identical pinhole, gain, and laser settings. Images in the medial and lateral VTA as well as the SN from the same tissue sections were acquired at the same focus level. The medial and lateral VTA was defined as the area that corresponds to the anatomical location of distinct DA subpopulations[4, 5]. The medial VTA was defined as the region comprising the medial paranigral nucleus (PN) and medial parabrachial pigmented nucleus (PBP), while the lateral VTA was defined as the lateral parabrachial pigmented nucleus (Supplementary Fig. 8c). No additional post-processing was performed on any of the collected images. ChR2 fluorescence intensity was then quantified using a scale from 0 – 255 in ImageJ to determine the mean intensity across the entire image. For retrobead, AAV and PHA-L injections as well as RV injections in the mPFC and

NAc lateral shell the injection-sites were confirmed in all animals by preparing coronal sections (100 μm). Counterstaining of injection sites was performed with green or red Nissl (NeuroTrace 500/525 or 530/615, Molecular Probes, Eugene, OR).

We routinely carried out complete serial analyses of the injection sites. Animals with significant contaminations outside target areas were discarded (see Lammel et al., 2008[4] for serial analysis of retrobead injection-sites and definition of DA target areas). For RV injections into the VTA we confirmed that all animals had the center of the viral injection located in the caudal VTA (Bregma -3.4 mm). However, quantification of the "spread" of the RV-ChR2 injected into the VTA is difficult because for expression of the transgene, the RV must be taken up by terminals and the transgene must be synthesized in the cytosol and then transported within the axons. Any EYFP within the VTA and adjacent structures will represent axons/terminals of cells that project to the VTA and adjacent structures as well as the cell bodies of neurons (i.e. RMTg) that have local connectivity within the VTA and adjacent structures. Thus transgene expression in structures adjacent to the VTA does not indicate that LHb or LDT neurons project to these structures. Nevertheless, in Supplementary Fig. 15 we present a serial reconstruction for the caudo-rostral extent of the midbrain showing the expression of ChR2-EYFP one week after injection of RV-ChR2 into the VTA (n=5 mice). TH-stained coronal midbrain sections (100 μM) were prepared from the injected mice and reconstructed using Neurolucida software (MicroBrightfield, Colchester, VT). Sections were labeled relative to bregma using landmarks and neuroanatomical nomenclature as described in the Franklin and Paxinos mouse brain atlas (2001). We report all brain areas in which detectable EYFP was observed. The strongest transgene expression was observed in the caudal VTA and several of its distinct subnuclei, most commonly in the interpeduncular nucleus (IPN). We also always detected high transgene expression in the RMTg. Thus when referred to in the text, the VTA includes the RMTg, which was originally termed the "tail of the VTA"[22].

Because the IPN expressed ChR2-EYFP following intra-VTA injections, we conducted additional double retrograde tracing experiments in which we injected small amounts of green Retrobeads (20 nl; LumaFlauor Inc., Naples, FL) into the IPN (bregma -3.9 mm; lateral 0 mm; ventral 4.55 mm) and red Retrobeads (60 nl; LumaFlauor Inc., Naples, FL) into the VTA (bregma -3.4 mm; lateral 0.35 mm; ventral 4.0 mm). Fluorescently-labeled latex Retrobeads were used in these experiments (n=2 mice) because they show very limited diffusion from the injection site even after several weeks *in vivo* and thus can be highly localized. While a large number of cells in the lateral habenula contained red beads (~84%, 79/94 cells), confirming a projection from this structure to the VTA, only a small proportion of these cells (~12%, 11/94 cells) also contained green beads (Supplementary Fig. 16). In contrast, a large number of medial habenula cells contained green beads (~98%, 214/218 cells) and less than 2% (3/218 cells) of these also contained red beads (Supplementary Fig. 16), demonstrating that the medial habenula preferentially projects to the IPN. In the LDT, many cells (>100) contained red beads and none of these cells contained green beads (Supplementary Fig. 16). These results suggest that LDT cells likely only project to VTA and not the IPN while the proportion of LHb neurons that project to the IPN in addition to the VTA is small.

For quantification of the expression of RV-ChR2-EYFP in the LDT and LHb 50 μm coronal sections from mice which had been injected with RV-ChR2-EYFP in the VTA were stained for NeuN. 66 confocal images from the LDT and 55 confocal images from the LHb were obtained using a 40X objective (n=3 mice). The percent of ChR2-EYFP-positive cells relative to the number of NeuN-positive cells in a 125 μm × 125 μm area was analyzed using the ImageJ software. Approximately 20% of all NeuN-positive LDT and LHb neurons expressed ChR2-EYFP following RV-ChR2 injection into the VTA (Supplementary Fig. 15).

## Behavioral Assays

All behavioral tests were conducted during the same circadian period (13:00 – 19:00). The conditioned place preference (CPP) and aversion (CPA) protocols were performed in a rectangular cage with a left chamber measuring 28 cm × 24 cm with black and white stripes on the walls and a metal grill floor, a center chamber measuring 11.5 cm × 24 cm with white walls and a smooth plastic floor; and a right chamber measuring 28 cm × 24 cm with black and white squares on the walls and a punched metal floor. The apparatus was designed so that mice did not have any consistent bias for a particular chamber (Supplementary Fig. 4b). The CPP/CPA test consisted of 3 sessions over 3 days. On day 1 (1 week after infusion of RV-EGFP or RV-ChR2 into the VTA), individual mice were placed in the center chamber and allowed to freely explore the entire apparatus for 15 min (pre-test). On day 2 mice were confined to one of the side chambers for 30 min during optical stimulation. Stimulation in left or right chambers was counter-balanced across mice. For stimulation the optical fiber was connected to a 473 nm laser diode (OEM Laser Systems, East Lansing, MI) through an FC/PC adapter. Laser output was controlled using a Master-8 pulse stimulator (A.M.P.I., Jerusalem, Israel) which delivered 8 pulses of 5 ms light flashes at 30 Hz every 5 s (phasic stimulation) or 5 ms light flashes delivered at 1 Hz (low frequency stimulation). For stimulation of LDT and LHb axon terminals in the VTA 15 pulses of 5 ms light flashes at 30 Hz every 2 s were delivered. Light output through the optical fibers was adjusted to 20 mW using a digital power meter console (Thorlabs, Newton, NJ) and was checked before and after stimulation of each mouse. On day 3, similar to day 1, mice were placed in the center chamber and allowed to freely explore the entire apparatus for 15 min (Post-Test 1). After Post-Test 1 the blue light laser was switched on and the mouse received phasic or low frequency stimulation for whenever it was in the chamber in which it had been conditioned on day 2 for a total duration of 15 min (Post-Test 2). There was no interruption between Post-Test 1 and Post-Test 2. A video tracking system (BiObserve, Fort Lee, NJ) recorded all animal movements. To calculate preference or aversion during Post-Test 1, we divided the relative time (in %) the mouse spent during Post-Test 1 in the conditioned chamber (i.e. the chamber in which it received either phasic or low frequency light stimulation of LDT or LHb inputs to the VTA) by the relative time (in %) the mouse spent in this chamber during the Pre-test (Post-Test 1 / Pre ratio). During Post-Test 2, preference or aversion was calculated by dividing the relative time (in %) the mouse spent during Post-Test 2 in the conditioned chamber by the relative time (in %) the mouse spent in this chamber during the Pre-test (Post-Test 2 / Pre ratio).

For microinjection of the D1 dopamine receptor antagonist SCH23390 into mPFC and the microinjection of the D1 and D2 dopamine receptor antagonists SCH23390 and raclopride into the NAc lateral shell a 33-gauge injector cannula connected to a syringe pump (Harvard Apparatus, MA) was inserted into the guide cannula which had been implanted in the mPFC or NAc lateral shell. All microinjections were delivered at a rate of 100 nl/min. Injector cannulas remained in place for an additional minute before being removed. Drugs were infused 5 min before the beginning of the light stimulation on day 2. For the pharmacological control experiments, the animals were treated identically except no optical stimulation was provided. Doses of drugs used for microinjections were: 50 ng SCH23390 in 0.2 μl saline (mPFC); 300 ng SCH23390 and 3 μg raclopride in 0.3 μl saline/DMSO (NAc lateral shell).

The open field test was conducted on different cohorts of mice to measure the effect of optogenetic stimulation on anxiety-like responses and general locomotor ability. The mice were placed in the chamber (50 × 50 cm) and their movement was recorded and analyzed for 18 min using the same video-tracking software that was used in the CPP/CPA tests (BiObserve, Fort Lee, NJ). After three minutes without optical stimulation, phasic stimulation was turned on for 3, three min epochs interspersed with 3 min epochs of no stimulation. For all analyses and graphs where total “off” and “on” conditions are displayed, the 3 “off” epochs were pooled and the 3 “on” epochs were pooled. The inner zone of the open field chamber was defined as the 23 × 23 cm central square area.

For quantification of c-fos immunreactivity, LDT and LHb inputs to the VTA were stimulated for 30 min using the phasic light stimulation protocol. During this time the mice remained in their home cage. The mice were perfused with 4% PFA 60 min after the *in vivo* light stimulation and 24h later immunohistochemistry was performed.

### Statistics

Student's t tests, Mann-Whitney U-tests or one-way ANOVA tests were used to determine statistical differences using GraphPad prism 5 (Graphpad Software, San Diego, CA). Bonferroni post hoc analysis was applied, when necessary, to compare means. Statistical significance was set at $p < 0.05$ (*), $p<0.01$ (**), $p<0.001$ (***). All data values are presented as means ± SEM.

## Supplementary Material

Refer to Web version on PubMed Central for supplementary material.

## Acknowledgements

We thank the Stanford Neuroscience Imaging Core, the Stanford Neuroscience Behavior Phenotyping and Pharmacology Core and the Stanford Neuroscience Gene Vector and Virus Core (all supported by NIH NS069375). We appreciate the constructive comments and experimental suggestions of the referees. This work was supported by grants from the Simons Foundation and NIH (to R.C.M.). K.D. is supported by the NIH, the DARPA REPAIR program, and the Wiegers Family Fund. S.L. is supported by a fellowship from the German Academy of Sciences Leopoldina. B.K.L. is supported by a Davis Foundation Postdoctoral Fellowship in Eating Disorders Research. K.M.T. is supported by the JPB Foundation and NIMH.

## References


1. Bjorklund A, Dunnett SB. Dopamine neuron systems in the brain: an update. Tr. Neurosci. 2007; 30:194–202.
2. Bromberg-Martin ES, Matsumoto M, Hikosaka O. Dopamine in motivational control: rewarding, aversive, and alerting. Neuron. 2010; 68:815–834. [PubMed: 21144997]
3. Schultz W. Multiple dopamine functions at different time courses. Annu. Rev. Neurosci. 2007; 30:259–288. [PubMed: 17600522]
4. Lammel S, et al. Unique properties of mesoprefrontal neurons within a dual mesocorticolimbic dopamine system. Neuron. 2008; 57:760–773. [PubMed: 18341995]
5. Lammel S, Ion DI, Roeper J, Malenka RC. Projection-specific modulation of dopamine neuron synapses by aversive and rewarding stimuli. Neuron. 2011; 70:855–862. [PubMed: 21658580]
6. Margolis EB, Mitchell JM, Ishikawa J, Hjelmstad GO, Fields HL. Midbrain dopamine neurons: projection target determines action potential duration and dopamine D(2) receptor inhibition. J. Neurosci. 2008; 28:8908–8913. [PubMed: 18768684]
7. Sesack SR, Grace AA. Cortico-Basal Ganglia reward network: microcircuitry. Neuropsychopharmacol. 2010; 35:27–47.
8. Geisler S, Derst C, Veh RW, Zahm DS. Glutamatergic afferents of the ventral tegmental area in the rat. J. Neurosci. 2007; 27:5730–5743. [PubMed: 17522317]
9. Berridge KC, Robinson TE, Aldridge JW. Dissecting components of reward: 'liking', 'wanting', and learning. Curr. Opin. Pharmacol. 2009; 9:65–73. [PubMed: 19162544]
10. Cohen JY, Haesler S, Vong L, Lowell BB, Uchida N. Neuron-type-specific signals for reward and punishment in the ventral tegmental area. Nature. 2012; 482:85–88. [PubMed: 22258508]
11. Guarraci FA, Kapp BS. An electrophysiological characterization of ventral tegmental area dopaminergic neurons during differential pavlovian fear conditioning in the awake rabbit. Behav. Brain Res. 1999; 99:169–179. [PubMed: 10512583]
12. Kim Y, Wood J, Moghaddam B. Coordinated activity of ventral tegmental neurons adapts to appetitive and aversive learning. PLoS One. 2012; 7:e29766. [PubMed: 22238652]
13. Tan KR, et al. GABA neurons of the VTA drive conditioned place aversion. Neuron. 2012; 73:1173–1183. [PubMed: 22445344]
14. Matsumoto M, Hikosaka O. Two types of dopamine neuron distinctly convey positive and negative motivational signals. Nature. 2009; 459:837–841. [PubMed: 19448610]
15. van Zessen R, Phillips JL, Budygin EA, Stuber GD. Activation of VTA GABA neurons disrupts reward consumption. Neuron. 2012; 73:1184–1194. [PubMed: 22445345]
16. Wickersham IR, Finke S, Conzelmann KK, Callaway EM. Retrograde neuronal tracing with a deletion-mutant rabies virus. Nat. Methods. 2007; 4:47–49. [PubMed: 17179932]
17. Watabe-Uchida M, Zhu L, Ogawa SK, Vamanrao A, Uchida N. Whole-brain mapping of direct inputs to midbrain dopamine neurons. Neuron. 2012; 74:858–873. [PubMed: 22681690]
18. Hikosaka O. The habenula: from stress evasion to value-based decision-making. Nat. Rev. Neurosci. 2010; 11:503–513. [PubMed: 20559337]
19. Forster GL, Blaha CD. Laterodorsal tegmental stimulation elicits dopamine efflux in the rat nucleus accumbens by activation of acetylcholine and glutamate receptors in the ventral tegmental area. Eur. J. Neurosci. 2000; 12:3596–3604. [PubMed: 11029630]
20. Lodge DJ, Grace AA. The laterodorsal tegmentum is essential for burst firing of ventral tegmental area dopamine neurons. Proc. Natl. Acad. Sci. USA. 2006; 103:5167–5172. [PubMed: 16549786]
21. Jhou TC, Geisler S, Marinelli M, Degarmo BA, Zahm DS. The mesopontine rostromedial tegmental nucleus: A structure targeted by the lateral habenula that projects to the ventral tegmental area of Tsai and substantia nigra compacta. J. Comp. Neurol. 2009; 513:566–596. [PubMed: 19235216]
22. Kaufling J, Veinante P, Pawlowski SA, Freund-Mercier MJ, Barrot M. Afferents to the GABAergic tail of the ventral tegmental area in the rat. J. Comp. Neurol. 2009; 513:597–621. [PubMed: 19235223]

23. Christoph GR, Leonzio RJ, Wilcox KS. Stimulation of the lateral habenula inhibits dopamine-containing neurons in the substantia nigra and ventral tegmental area of the rat. J. Neurosci. 1986; 6:613–619. [PubMed: 3958786]
24. Jhou TC, Fields HL, Baxter MG, Saper CB, Holland PC. The rostromedial tegmental nucleus (RMTg), a GABAergic afferent to midbrain dopamine neurons, encodes aversive stimuli and inhibits motor responses. Neuron. 2009; 61:786–800. [PubMed: 19285474]
25. Ji H, Shepard PD. Lateral habenula stimulation inhibits rat midbrain dopamine neurons through a GABA(A) receptor-mediated mechanism. J. Neurosci. 2007; 27:6923–6930. [PubMed: 17596440]
26. Omelchenko N, Bell R, Sesack SR. Lateral habenula projections to dopamine and GABA neurons in the rat ventral tegmental area. Eur. J. Neurosci. 2009; 30:1239–1250. [PubMed: 19788571]
27. Araki M, McGeer PL, Kimura H. The efferent projections of the rat lateral habenular nucleus revealed by the PHA-L anterograde tracing method. Brain Res. 1988; 441:319–330. [PubMed: 2451982]
28. Cornwall J, Cooper JD, Phillipson OT. Afferent and efferent connections of the laterodorsal tegmental nucleus in the rat. Brain Res. Bull. 1990; 25:271–284. [PubMed: 1699638]
29. Vertes RP, Fortin WJ, Crane AM. Projections of the median raphe nucleus in the rat. J. Comp. Neurol. 1999; 407:555–582. [PubMed: 10235645]
30. Sanchez CJ, Bailie TM, Wu WR, Li N, Sorg BA. Manipulation of dopamine d1-like receptor activation in the rat medial prefrontal cortex alters stress- and cocaine-induced reinstatement of conditioned place preference behavior. Neuroscience. 2003; 119:497–505. [PubMed: 12770563]
31. Tsai HC, et al. Phasic firing in dopaminergic neurons is sufficient for behavioral conditioning. Science. 2009; 324:1080–1084. [PubMed: 19389999]
32. Witten IB, et al. Recombinase-driver rat lines: tools, techniques, and optogenetic application to dopamine-mediated reinforcement. Neuron. 2011; 72:721–733. [PubMed: 22153370]
33. Robbins TW, Arnsten AF. The neuropsychopharmacology of fronto-executive function: monoaminergic modulation. Annu. Rev. Neurosci. 2009; 32:267–287. [PubMed: 19555290]
34. Lecourtier L, Defrancesco A, Moghaddam B. Differential tonic influence of lateral habenula on prefrontal cortex and nucleus accumbens dopamine release. Eur. J. Neurosci. 2008; 27:1755–1762. [PubMed: 18380670]
35. Li B, et al. Synaptic potentiation onto habenula neurons in the learned helplessness model of depression. Nature. 2011; 470:535–539. [PubMed: 21350486]
36. Lecourtier L, Kelly PH. Bilateral lesions of the habenula induce attentional disturbances in rats. Neuropsychopharmacol. 2005; 30:484–496.
37. Shepard PD, Holcomb HH, Gold JM. Schizophrenia in translation: the presence of absence: habenular regulation of dopamine neurons and the encoding of negative outcomes. Schizophr Bull. 2006; 32:417–421. [PubMed: 16717257]
38. Zhang F, et al. Optogenetic interrogation of neural circuits: technology for probing mammalian brain structures. Nat. Protoc . 2010; 5:439–456. [PubMed: 20203662]
39. Mebatsion T, Konig M, Conzelmann KK. Budding of rabies virus particles in the absence of the spike glycoprotein. Cell. 1996; 84:941–951. [PubMed: 8601317]
40. Wickersham IR, Sullivan HA, Seung HS. Production of glycoprotein-deleted rabies viruses for monosynaptic tracing and high-level gene expression in neurons. Nat. Protoc. 2010; 5:595–606. [PubMed: 20203674]

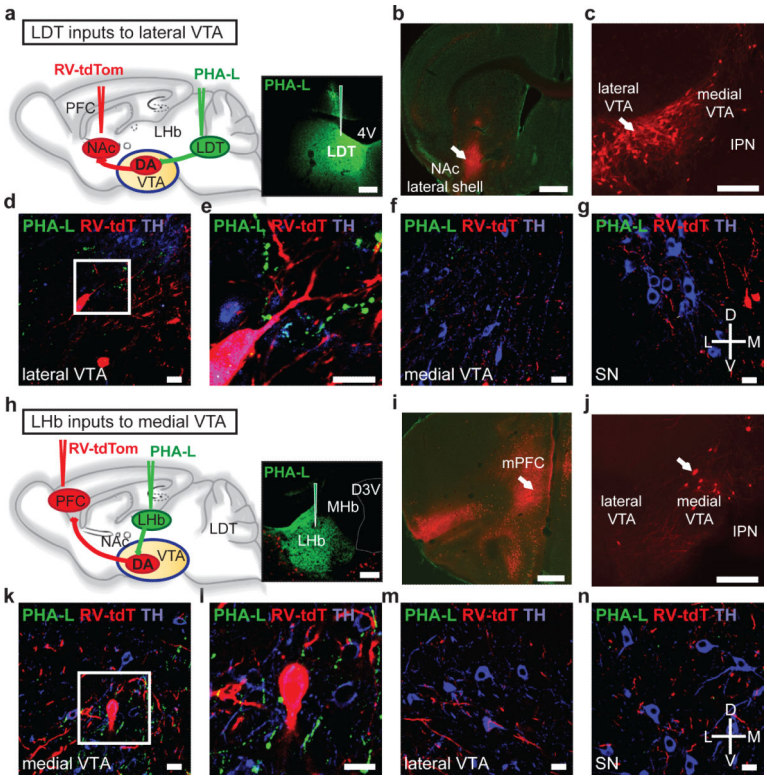


**Figure 1. LDT and LHb preferentially project to distinct VTA subregions**

**a**, Injection sites for RV-tdTomato in NAc and PHA-L in LDT. Image shows PHA-L staining in LDT (4V: fourth ventricle). **b**, RV-tdTomato in NAc lateral shell. **c**, VTA neurons projecting to NAc lateral shell are mainly located in lateral VTA (IPN: interpeduncular nucleus) (a-c scale bars, 200 μm). **d,e**, PHA-L labeled terminals (green) from LDT are adjacent to cells projecting to NAc lateral shell (red) as well as TH-immunopositive processes (blue). **f, g**, Few PHA-L labeled terminals were detected in medial VTA (**f**) and in SN (**g**) (d-g scale bars, 20 μm). **h**, Injection sites for RV-tdTomato in mPFC and PHA-L in LHb. Image shows PHA-L staining in LHb (MHb: medial habenula; D3V: dorsal third ventricle). **i**, RV-tdTomato in mPFC. **j**, VTA neurons projecting to mPFC are mainly located in medial VTA (h-j scale bars, 200 μm). **k, l**, PHA-L labeled terminals (green) from LHb are found adjacent to cells projecting to mPFC (red) as well as TH-immunopositive processes (blue). **m, n**, Few PHA-L labeled terminals were detected in lateral VTA (**m**) and in SN (**n**) (k-n scale bars, 20 μm).

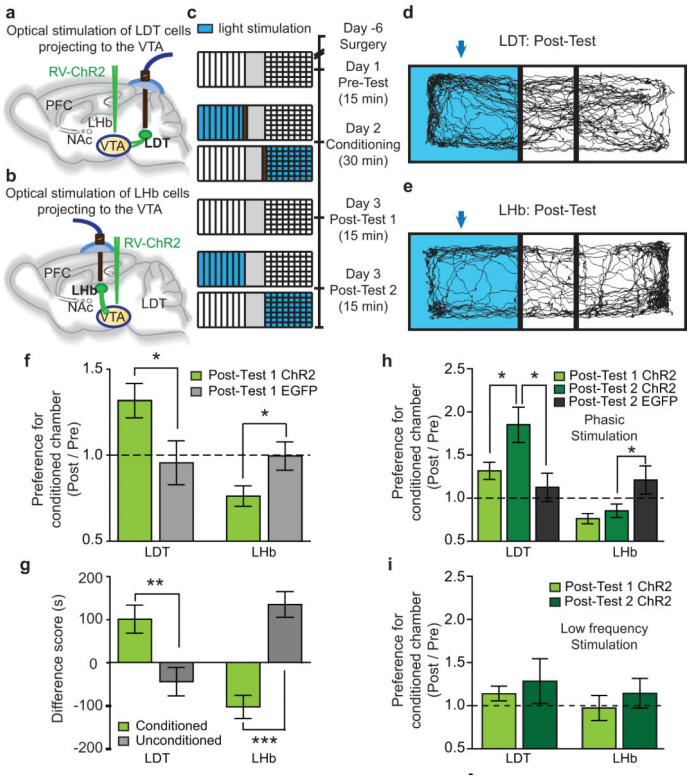


**Figure 2. Stimulation of LDT and LHb inputs to VTA elicits CPP and CPA**

**a,b**, RV-ChR2 injection into VTA and optical stimulation of (**a**) LDT- and (**b**) LHb projection neurons. **c**, Procedure to elicit and test CPP and CPA. **d,e**, Example day 3 mouse tracks, Post-Test 1. Arrow indicates chamber in which (**d**) LDT or (**e**) LHb projection neurons were stimulated on Day 2. **f**, Ratio from Post-Test1/Pre-Test of time spent in conditioned chamber was higher in LDT-ChR2 mice compared to LDT-EGFP mice (LDT-ChR2: 1.32 ± 0.1, n=8; LDT-EGFP: 0.96 ± 0.13, n=7) but lower in LHb-ChR2 mice (LHb-ChR2: 0.76 ± 0.06, n=9; LHb-EGFP: 0.99 ± 0.08, n=11). **g**, Differences between Post-Test 1 and Pre-Test in time mice spent in conditioned or unconditioned chambers. (LDT-ChR2 mice: conditioned chamber: 105.4 ± 34.38, n=8; unconditioned chamber: -51.1 ± 26.76, n=8) (LHb-ChR2 mice: cond. chamber: -90.87 ± 22.59, n=9; unconditioned chamber: 124.3 ± 26.27, n=9). **h**, Stimulation of LDT-ChR2 mice during Post-Test 2 enhanced preference for conditioned chamber (LDT-ChR2 Post-Test 1, 1.32 ± 0.1, n=8; Post-Test 2, 1.85 ± 0.2, n=8; Post-Test 2 LDT-EGFP mice 1.13±0.16, n=7). Stimulation of LHb-Chr2 mice during Post-Test 2 did not cause further aversion (LHb-ChR2 Post-Test 1, 0.76 ± 0.06, n=9; Post-Test 2, 0.85±0.08, n=9) which was still present (LHb-EGFP Post-Test 2, 1.22±0.16, n=11). (Post-test 1 results are same as in f). **i**, Low frequency stimulation of LDT-ChR2 and LHb-ChR2 cells did not elicit CPP or CPA (Post-Test 1, LDT-ChR2, 1.13 ± 0.09, n=6; Post-Test 2, LDT-ChR2, 1.28 ± 0.26, n=6; Post-Test 1, LHb-ChR2, 0.97 ± 0.14, n=7; Post-Test 2, LHb-ChR2, 1.14 ± 0.17, n=6). Error bars denote s.e.m. *p<0.05; **p<0.01; ***p<0.001, Mann-Whitney U-test.

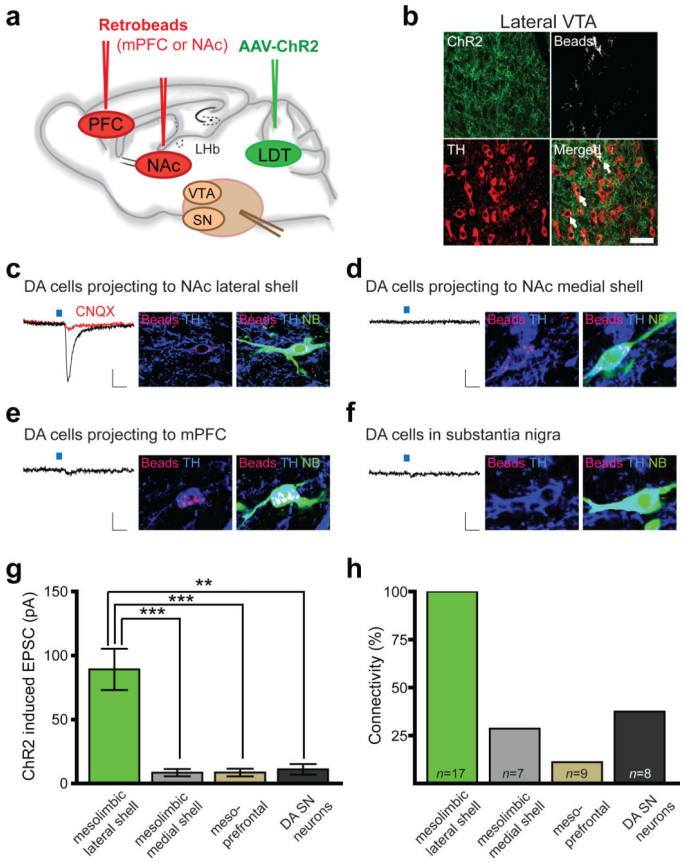


**Figure 3. LDT neurons preferentially synapse on DA neurons projecting to NAc lateral shell**

**a**, AAV-ChR2-EYFP injected into LDT and retrobeads injected into NAc lateral shell and NAc medial shell or in mPFC. **b**, ChR2-EYFP expression in close proximity to retrogradely labeled (beads) TH-immunopositive neurons in lateral VTA (scale bar, 50 μm). **c-f**, Traces from whole-cell recordings at -70 mV showing EPSCs generated by stimulation of LTD inputs in retrogradely labeled VTA neurons (beads) projecting to (**c**) NAc lateral shell, (**d**) NAc medial shell, (**e**) mPFC or (**f**) SN neurons. All cells were filled with neurobiotin (NB, green) and are TH-immunopositive (blue). Scale bars: 20 pA/20 ms. **g**, Summary of average EPSCs generated by optical stimulation of LDT inputs in the four cell populations ( **p<0.01, ***p<0.001, 1 way ANOVA with Bonferroni post-hoc test; Error bars denote s.e.m.). **h**, Percentage of cells in which optical stimulation generated EPSCs >10 pA. N's shown within each bar also apply to g.

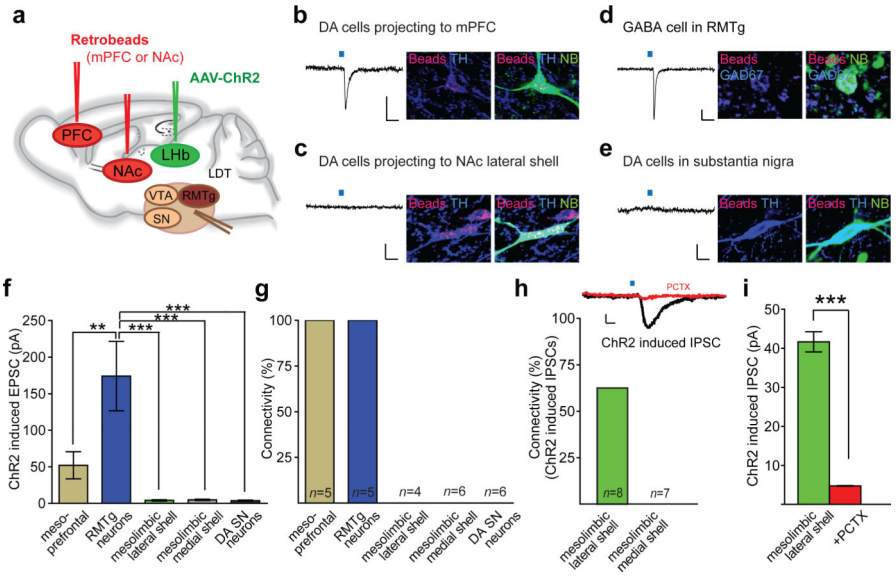


**Figure 4. LHb neurons preferentially synapse on DA neurons projecting to mPFC and RMTg GABAergic neurons**

**a**, AAV-ChR2-EYFP injected into LHb and retrobeads injected either into NAc lateral shell and NAc medial shell or in mPFC. **b-e**, Traces from whole-cell recordings at -70 mV showing EPSCs generated by optical stimulation of LHb inputs in retrogradely labeled VTA neurons (beads, red) projecting to (**b**) mPFC or (**c**) NAc lateral shell or (**d**) an RMTg cell and (**e**) SN cell. All cells were filled with neurobiotin (NB, green) and are either TH-immunopositive (blue) (**b, c, e**) or GAD67-immunopositive (blue, **d**). Scale bars: 20 pA/20 ms. **f**, Summary of average EPSCs generated by optical stimulation of LHb inputs in five cell populations ( **p<0.01, ***p<0.001, 1 way ANOVA with Bonferroni post-hoc test, error bars denote s.e.m.). **g**, Percentage of cells in which optical stimulation generated EPSCs >10 pA. N's shown in this graph also apply to f. **h**, Optical stimulation of LHb inputs generates IPSC in DA cell projecting to NAc lateral shell (PCTX, picrotoxin) (scale bars, 20 pA/20 ms). Graph shows percentage of DA cells projecting to NAc lateral shell or medial shell in which IPSCs were generated by LHb input stimulation. **i**, Average IPSC size from DA cells projecting to NAc lateral shell. IPSCs were blocked by picrotoxin (n=3; ***p<0.0001, unpaired Student's t-test).

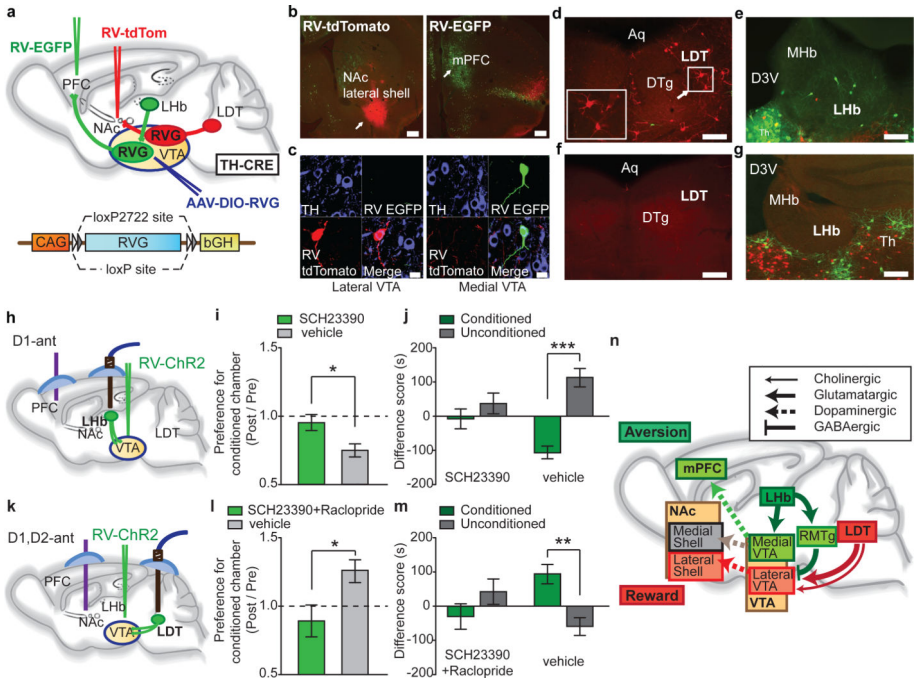


**Figure 5. Rabies virus reveals distinct VTA circuits and effects of DA receptor antagonists on CPP/CPA**

**a**, AAV expressing rabies glycoprotein (RVG) in a Cre-dependent manner was injected into VTA of TH-Cre mice. RV-EGFP and RV-tdTomato, injected subsequently into mPFC and NAc, respectively, are retrogradely transported to subpopulations of DA neuron in which transcomplementation occurs, allowing RV to spread retrogradely and label cells that synaptically contact infected DA neurons. **b**, Injection sites in NAc lateral shell (RV-tdTomato) and mPFC (RV-EGFP) (scale bars, 200 μm). **c**, TH-immunoreactive neurons in VTA retrogradely labeled by RV-tdTomato or RV-EGFP (scale bars, 20 μm). **d,e** tdTomato and EGFP labeling in LDT (**d**) and LHb (**e**) neurons, respectively, when injection of AAV-DIO-RVG into VTA of TH-Cre mice was performed prior to RV injections (DTg, dorsal tegmental nucleus; Aq, aqueduct; MHb, medial habenula; D3V, dorsal third ventricle; Th, thalamus) (d, e scale bars, 100 μm). **f,g**, Lack of tdTomato expression in LDT (**f**) and lack of EGFP expression in LHb (**g**) following RV injections in TH-Cre mice that were not injected with AAV-DIO-RVG (f, g scale bars, 100 μm). **h**, Placements of drug infusion cannula into mPFC and optic fiber into LHb as well as injection of RV-ChR2 into VTA. **i**, Ratio of Post-Test/Pre-Test time spent in conditioned chamber when SCH23390 (SCH) or vehicle was infused into mPFC prior to LHb optical stimulation (SCH: 0.95 ± 0.05, n=9; vehicle: 0.75 ± 0.04, n=7). **j**, Difference between Post-Test and Pre-Test in time mice spent in conditioned or unconditioned chambers following LHb stimulation (SCH: conditioned chamber, -7.24 ± 28.79, unconditioned chamber: 36.83 ± 30.74, n=9; vehicle: conditioned chamber, -106.88 ± 18.82, unconditioned chamber, 112.61 ± 26.48, n=7). **k**, Placements of drug infusion cannula into NAc lateral shell and optic fiber into LDT as well as injection of RV-ChR2 into VTA. **l**, Ratio of Post-Test /Pre-Test time spent in conditioned chamber when SCH23390 and raclopride (rac) or vehicle were infused into NAc lateral shell prior to LDT optical stimulation (SCH/rac: 0.89 ± 0.1, n=7; vehicle:1.26 ± 0.08, n=6). **m**, Difference between

Post-Test and Pre-Test in time mice spent in conditioned or unconditioned chamber following LDT stimulation (SCH/rac: conditioned chamber: -30.17 ± 37.38, unconditioned chamber: 42.22 ± 34.68, n=7; vehicle: conditioned chamber: 94.58 ± 27.77, unconditioned chamber, -59.38 ± 26.44, n=6) *p<0.05, **p<0.01, ***p<0.001, Mann-Whitney U-test. Error bars denote s.e.m. **n**, Hypothesized circuits driven by LDT and LHb inputs into the VTA. Green shading indicates circuit involved in aversion; red/pink shading indicates circuit involved in reward and salience.